Structural Characterization of the Ag/Ca Transparent Electrode for Organic Light Emitting Diodes

Boo Kyung Kim[1], Yang Hwi Cho[1], Byung Tae Ahn[1,*], and Dae Gyu Moon[2]

[1]Department of Materials Science and Engineering, KAIST, Daejeon 305-701, Korea
[2]Department of Materials Engineering, Soonchunhyang University, Asan, Chungnam 336-745, Korea

The Ag/Ca double layer, a candidate material for a transparent cathode in top-emitting organic light emitting diodes, becomes semitransparent upon exposure to air. It was found that the bottom Ca layer becomes a $Ca(OH)_2$ layer, and the top Ag layer becomes an Ag (35% Ca) layer. The origin of the higher transmittance of the Ag/Ca double layer compared to the Ag single layer is explained as follows: The oxidation of the Ca layer to $Ca(OH)_2$ leads to compressive stress on the bottom layer and tensile stress on the top layer. Due to the stress gradient, the unreacted Ca in the bottom layer is pushed into the top Ag layer to form a Ag-Ca solid solution, reducing the conductivity in the top layer and increasing the transmittance of the top layer. A high-transmittance and low-resistivity top electrode can be designed when the Ag layer is connected continuously and it partially covers the surface of the bottom layer.

Keywords: OLED, transparent electrode, Ag/Ca electrode

1. INTRODUCTION

Among flat panel display technologies, the liquid crystal display (LCD) is currently the dominant technology due to its light weight, low power consumption, and ease of operation. LCDs have drawbacks, however, related to their view angle, response time, and brightness. The organic light-emitting diode (OLED) display has the potential to resolve these issues with LCD-based displays. However, as OLED technology employs a current driving method for device operation, active-matrix OLED needs additional thin-film transistors (TFTs) compared to LCD, resulting in a reduced light-emitting area for each pixel. To increase the aperture ratio, a top-emission OLED that is unaffected by the number of TFTs may meet the requirements. For this purpose, technologies related to a stable reflective anode, a transparent cathode, and transparent encapsulation should be achieved.[1-4]

A proper cathode requires the use of metals with a low work function in order to simplify the electron injection from the metal to the organic LED. Such metals include Al, Mg, Ca, Ag, Mg:Ag, and LiF:Al.[5, 6] However, because metals with a low work function are always susceptible to atmospheric oxidation, low-work-function metals with a protective layer or alloys with stable metals having a relatively high work function are generally used for the cathode. Ca is

suitable for use with high electron injection due to its low work function (2.9~3.0 eV), and Ag is suitable as a protective layer for the reactive Ca due to its high stability and ease of deposition. From the Ag/Ca double layer, it was reported that the electrode becomes semitransparent,[7,8] and hence this electrode has been applied to OLED devices as a top-emission electrode.[9,10]

Even though the Ag/Ca double layer has already been applied to OLED devices, the exact structure of the Ag/Ca double layer is not completely understood. In this study, the structure and optical properties of the Ag/Ca double layer have been systematically studied, and an explanation of the increased transmittance in the Ag/Ca double layer compared to a Ag single layer has been found.

2. EXPERIMENT

99.99% purity Ag and 99.5% purity Ca were obtained from Kojima Chemicals Co. and Junsei Co., respectively. Using these chemicals as evaporation sources, an Ag/Ca double layer was deposited via vacuum thermal evaporation at 4×10^{-7} torr with a deposition rate of 1 Å/s onto a glass substrate, a Si oxide wafer, or a Si wafer. Before the Ag layer was deposited, the deposition was paused for approximately 10 min. As two tungsten boats were used, there was no vacuum break between the Ca deposition and the Ag deposition. The thickness of the film was controlled by a quartz crystal monitor (QCM). The substrate was rotated

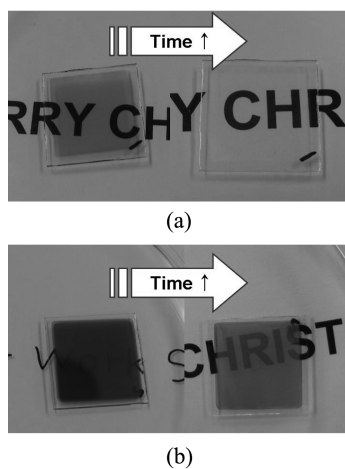*Corresponding author: btahn@kaist.ac.kr

during the deposition to improve the uniformity of the film.

A four-point probe was used to measure the resistivity and sheet resistance. A UV spectrometer was used to obtain the optical transmission spectra in a wavelength of 380 to 780 nm. A scanning electron microscope (SEM) was used to examine the thickness and the surface morphology of the deposited films. X-ray diffraction (XRD) using Cu Kα radiation of $\lambda = 1.5405$ was used to characterize the phase and crystal structure. It was operated at 40 kV and 100 mA at a scan speed of 2.4°/min and an incident angle of 1.5°. A depth profile by an Auger electron spectroscope (AES) was utilized to investigate the compositional variance and the structure of the deposited films. A sample was prepared using a focused ion beam microscope (FIM) and the crystal structure and microstructure image of the film were analyzed using transmission electron microscopy (TEM).

3. RESULTS

Figure 1(a) shows the transparency change of the Ca single layer deposited onto a glass substrate. The Ca layer was gray in the vacuum. When the thickness of the Ca layer was less than 70 nm, it became transparent almost immediately in air. In contrast, when the thickness was 70 nm or over, the change from gray to transparency was relatively slow upon exposure to air. Figure 1(b) shows the transparency of the Ag/Ca double layer. The initial color was black and the layer became semitransparent. When a single layer of Ag was deposited, the Ag was opaque and the transparency did not change.

Figure 2 shows SEM micrographs of (a) Ag (10 nm), (b) Ca (10 nm), and (c) Ag (10 nm)/Ca (10 nm) deposited onto a glass substrate. On a glass substrate, the Ag film was not well connected, as shown in Fig. 2(a), while a uniform and continuous Ca film formed, as shown in Fig. 2(b). This suggests that Ca is highly adhesive on a glass substrate, while

Ag is not adhesive. When Ag was deposited on a Ca layer, the Ag was continuous and uniform, as seen in Fig. 2c, suggesting that Ag is adhesive to Ca.

In Fig. 2(a), the white area is Ag metal and the dark area is glass. The Ag area in the figure is shiny due to the high reflectance of the Ag metal. The brightness of Ca in Fig. 2(b) is low due to the low reflectance of the Ca metal. In Fig. 2(c), despite the fact that the top layer is Ag, the brightness is low compared to that of Fig. 2(a), suggesting that an Ag/Ca double layer has less reflectivity than a silver single layer. In other words, the Ag/Ca double layer has higher transmittance than the Ag single layer.

Figure 3 shows the spectroscopic response of the transmit-

(a)

(b)

(c)
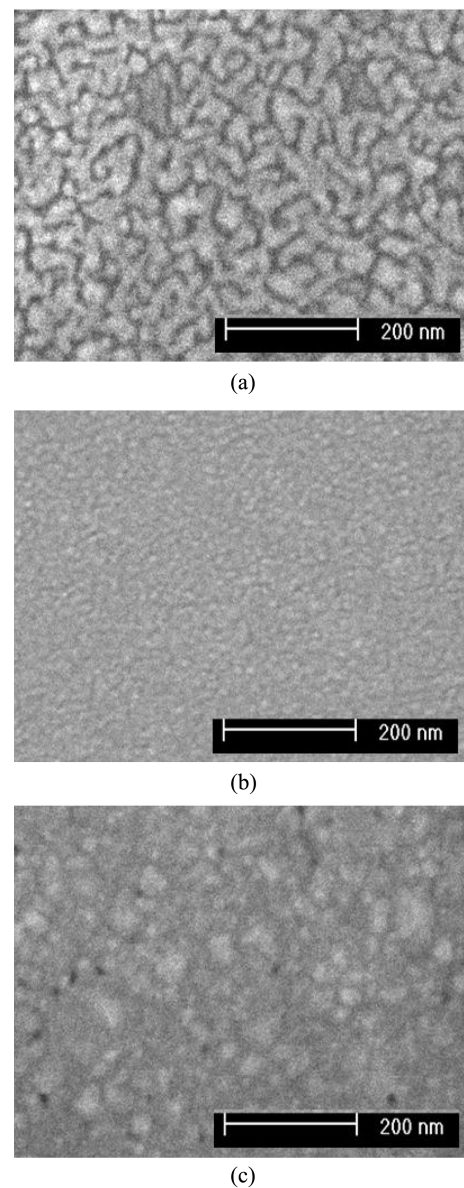
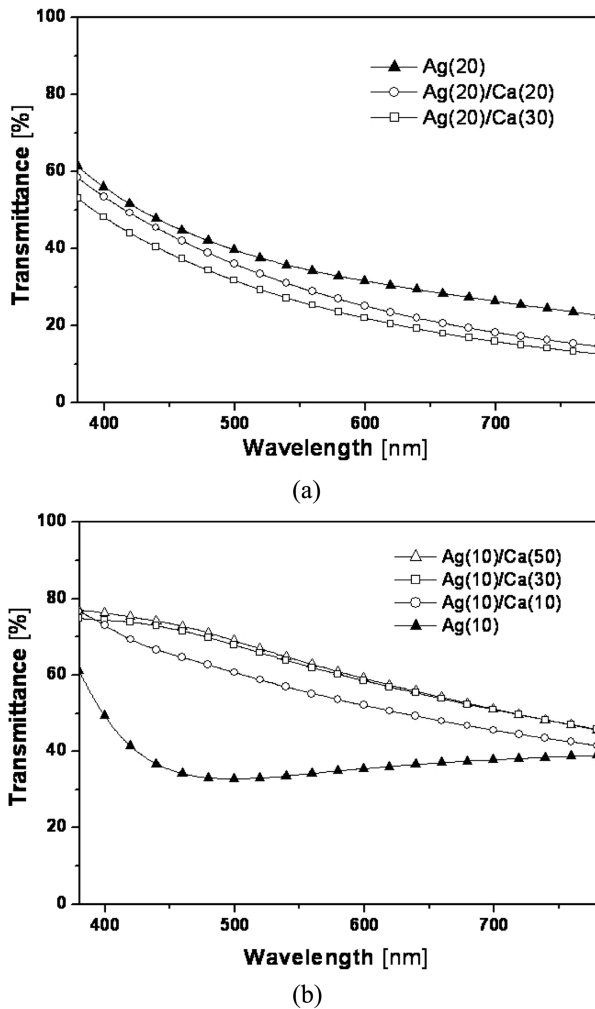**Fig. 2.** SEM micrographs of (a) Ag(10 nm)/glass, (b) Ca(10 nm)/glass, and (c) Ag(10 nm)/Ca(10 nm)/glass.

(a)

(b)

Fig. 1. Transparency change over time of (a) a Ca single layer and (b) a Ag/Ca double layer.

(a)

(b)

Fig. 3. The spectroscopic response of transmittance of (a) a Ag(20 nm)/Ca double layer and (b) a Ag(10 nm)/Ca double layer.

Fig. 4. XRD patterns of (a) a Ag(10 nm)/Ca(150 nm) double layer on a glass substrate, (b) the as-deposited Ca on a TiN substrate and (C) Ca on a TiN substrate after annealing at 200°C in air.

tance of the Ag/Ca double layer. Two features are noticeable in this figure. First, the continuity of the Ag film affects the shape of the spectroscopic transmittance. In Fig. 3(a), where the 20-nm-thick single Ag layer on glass is a continuous film, the transmittance monotonically decreases as the wavelength increases due to free-carrier scattering. In Fig. 3(b), the 10-nm-thick single Ag layer on glass is not continuous (also see Fig. 2(a)), and the shape of the spectroscopic response is very different. The transmittance drops rapidly at short wavelengths up to 450 nm and then slightly increases as the wavelength increases. The reason for the increase in transmittance is less free-carrier scattering, as this is limited by the geometrical confinement of the free carriers within the Ag islands.

Second, in the Ag/Ca double layer, the transmittance is lowered as the thickness of the Ca layer increases when the Ag thickness is 20 nm (Fig. 2(a)). This is normal, because the light absorption increases as the thickness of the material
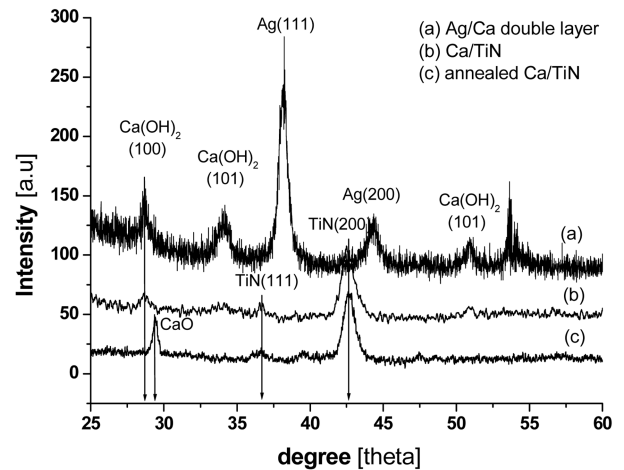
increases. However, when the Ag thickness is 10 nm, the transmittance is increased as the Ca thickness increases from 10 to 30 nm (Fig. 2(b)). The transmittance with 50-nm-thick Ca is similar to that with 30-nm-thick Ca.

Given that the Ag layers are continuous in both cases, the increase in transmittance for a double layer with 10-nm-thick Ag is an unexpected result: in general, the transmittance is smaller as the film thickness increases. It is an intriguing question as to why the transmittance of the Ag (10 nm)/Ca double layer is higher than that of the Ag single layer.[11] This phenomenon is explained in a subsequent part of this study.

Figure 4 shows XRD patterns of (a) an Ag/Ca double layer on a glass substrate exposed to air, (b) a Ca layer on a TiN substrate exposed to air, and (c) a Ca layer on a TiN substrate after thermal annealing at 200°C in air or Ar. The thicknesses of the Ag and Ca are 10 and 150 nm, respectively. For the Ag/Ca double layer, the XRD peaks are identified as those of Ag and $Ca(OH)_2$. For the Ca single layer on TiN, the peak is also identified as $Ca(OH)_2$.[12,13] When the Ca on TiN is annealed in air or Ar, the $Ca(OH)_2$ changes to CaO. The results of this investigation indicate that Ca metal is oxidized to $Ca(OH)_2$ in air due to moisture. If the Ag/Ca double layer is exposed in a moisture-free air, it is very likely that the Ca is oxidized to CaO, although the process is very slow because the dissociation of O_2 requires more time compared to that of H_2O.[14] The lattice constant of the Ag metal in the double layer is 0.427 nm. This shows an increase from that of pure Ag of 0.408 nm, suggesting that the lattice parameter was significantly increased by means of Ca incorporation, which is discussed in the next paragraph.

Figure 5 shows the AES depth profile of the Ag (10 nm)/ Ca (30 nm) double layer exposed in air. The top region has a high Ag content, and the bottom layer has no Ag in it. One
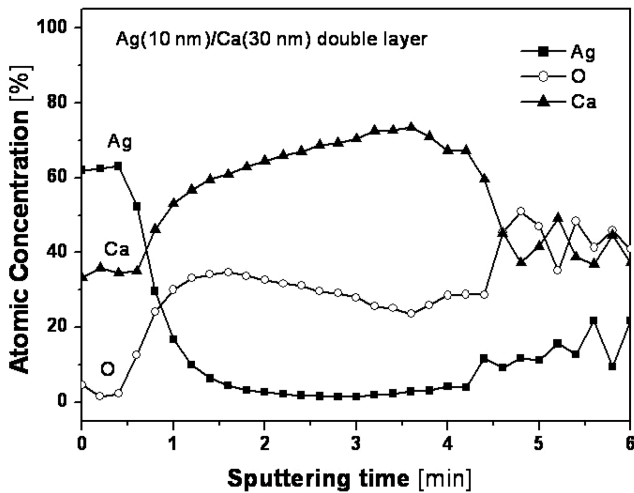
**Fig. 5.** AES depth profile of the Ag(10 nm)/Ca(30 nm) double layer.

noticeable feature in the top layer is that Ca is present in uniform concentrations. The Ca content of 35% in the layer, a large value, is also an interesting finding. Moreover, no appreciable amount of oxygen is found in the top layer, although the Ca content is high in the region. This indicates that the Ca in the top layer is not oxidized and remains in the form of Ca metal. The Ca content in the top layer was nearly constant for Ag(10 nm)/Ca(10 nm), Ag(10 nm)/Ca(30 nm), Ag(10 nm)/Ca(50 nm), and Ag(50 nm)/Ca (30 nm).

In contrast to the aforementioned findings, the Ca metal in the region was not detected by an XRD analysis (Fig. 4), suggesting that Ca exists as either a solid solution in Ag or an amorphous state. As Ca is highly reactive with moisture or oxygen, amorphous Ca will become $Ca(OH)_2$ or CaO.[12] Therefore, the existence of pure Ca in a metal state or a glass state can be excluded. If the top layer is in the Ag-Ca alloy amorphous state, the XRD pattern will show a broad peak. No such peak was observed, however, indicating that the top layer is not in an amorphous state. Thus, it is believed that the Ca in the Ag layer exists as a solid solution, as the lattice parameter of the Ag alloy increased from 0.408 to 0.427 nm. The solubility of Ca in Ag is very small in a bulk material; however, the top layer has tensile stress due to the volume expansion of the bottom layer, which increases the solubility of the Ca into Ag through Ag crevices. The Ca solubility in the top layer is approximately 35%.

Ca and O are found in the bottom layer, because the Ca layer is transformed to $Ca(OH)_2$ via the diffusion of moisture or oxygen through the top layer. The oxygen content is nearly 35% and is slightly less near the glass substrate, most likely due to the rigid-substrate constraint. The Ca content continuously varies from nearly 50% near the interface to nearly 70% near the glass substrate. The profile clearly indicates that some Ca has diffused out from the bottom layer to the top layer.
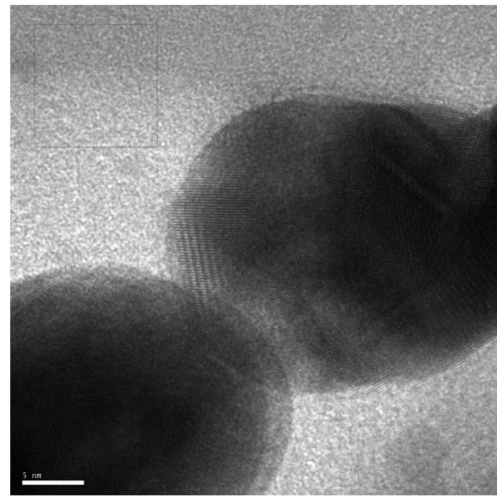
(a)
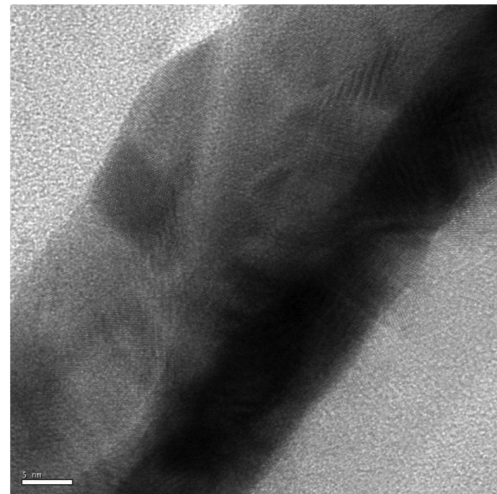
(b)

Fig. 6. The cross-sectional TEM images of (a) Ag(10 nm) and (b) Ag(10nm)/Ca(10 nm) on a glass substrate.

Figure 6 shows cross-sectional TEM images of (a) Ag (10 nm) and (b) Ag(10 nm)/Ca (10 nm) on a glass substrate. In Fig. 6(a), the dark area is Ag, and the white area is glass. When pure Ag is deposited, the Ag is clustered with a thickness larger than 10 nm, leading to lower optical transmittance. In Fig. 6(b), the dark area is the Ag(Ca) layer and the gray area is the $Ca(OH)_2$ layer. The thickness of the Ag(Ca) layer is fairly uniform and no noticeable morphology change has been found. Given a Ca content in the Ag layer of nearly 35%, there are many reasons for such a high content, for example by a AgCa intermediate alloy compound or a Ag-Ca amorphous phase. From the TEM image, however, no significant amorphous state or new compound can be seen.

Based on the above analysis, Fig. 7 shows a schematic explanation of the phase change in the Ag/Ca double layer upon exposure to air. In a vacuum, the Ag/Ca double layer is
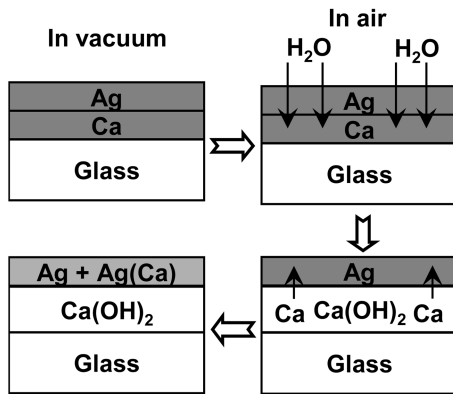
Fig. 7. The schematic explanation of the phase change in the Ag/Ca double layer.

formed through thermal evaporation (Fig. 7(a)). When the sample is exposed to air, the moisture in air is diffused through the Ag layer and reacts with Ca to form $Ca(OH)_2$ (Fig. 7(b)). Due to the volume expansion by oxidation in the bottom layer, the bottom layer is under compressive stress and the top layer is under tensile stress. As a result, the unreacted Ca metal is pushed out from the bottom layer to the top layer, forming a Ag-Ca solid solution with a high Ca content (Fig. 7(c)).

One of the most intriguing phenomena in the Ag/Ca double-layer electrode is that the transmittance of the Ag/Ca double layer is much higher than that of a uniform Ag single layer, even with an Ag thickness of 10 nm. This does not apply to the Ag(20 nm)/Ca(10 nm) double layer, as the moisture in air cannot pass through the 20-nm thick Ag layer. The key to understanding the phenomenon is the formation of the transparent $Ca(OH)_2$ bottom layer and less opaque Ag(Ca) top layer.[13,14] To understand the physics behind this phenomenon, it is necessary to consider the optical absorption coefficient in metals: the lower the absorption coefficient, the higher the optical transmittance. The absorption coefficient in metals is affected by free-carrier scattering, and it is proportional to $(\sigma_o\lambda)^{1/2}$, where σ_o is the dc electrical conductivity and λ is the light wavelength.[15] The absorption coefficient decreases if the dc conductivity decreases due to less free-carrier scattering. The sheet resistance of 10-nm-thick Ag(Ca) film is about 9.6 $\Omega/\square$, resulting in the conductivity of $1.0\times10^5/\Omega\cdot cm$. Since the conductivity of pure Ag metal is $6.2\times10^5/\Omega\cdot cm$, the absorption coefficient of the Ag(Ca) layer is lowered, and the transmittance is increased due to less free-carrier scattering.

Based on the above analysis, it is possible to design an optimum Ag/Ca double layer with high transmittance and high electrical conductivity. For this purpose, the surface coverage of the Ag layer should be as low as possible as far as it is a continuous film. In this case, the top layer consists of both an Ag(Ca) solid solution and $Ca(OH)_2$ phases. Due to
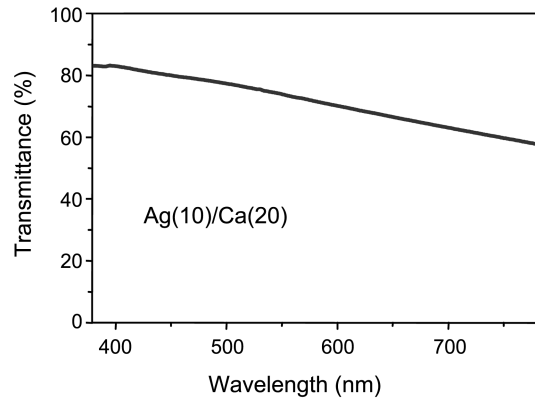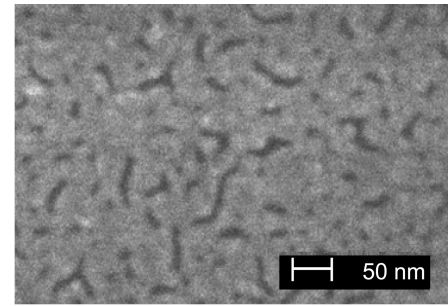

Fig. 8. An SEM image of the microstructure and transmittance of Ag(7 nm)/Ca(20 nm).

the areas with the transparent $Ca(OH)_2$ phase, the transmittance increases. Figure 8 shows an SEM image of the microstructure of an Ag (7 nm)/Ca (20 nm) film and its high transmittance. The Ag (Ca) top layer is not completely covered, but it is continuous, leading to good electrical conductivity. The dark area in the SEM image consists of the transparent $Ca(OH)_2$ phase. The sheet resistance and transmittance of the film are 13 $\Omega/\square$ and approximately 80% at 500-nm wavelength, respectively.

4. CONCLUSIONS

The Ag/Ca double layer becomes semitransparent upon exposure to air when the thickness of the Ag layer is below 10 nm. Under air exposure, it was found that the Ca in the Ag/Ca double layer became a $Ca(OH)_2$ phase and that the Ag became an Ag(Ca) solid solution with a Ca content of 35%. The lattice constant of the Ag phase increased from 0.408 nm to 0.427 nm as a result of Ca incorporation. The $Ca(OH)_2$ phase became CaO after annealing at 200°C in air or Ar.

The structural change in the Ag/Ca double layer under air exposure can be explained as follows: When the Ag/Ca double layer is exposed to air, the moisture in the air diffuses through the Ag layer and reacts with Ca to form $Ca(OH)_2$. Due to the volume expansion by oxidation in the bottom layer, the bottom layer undergoes compressive stress and the

top layer undergoes tensile stress. As a result, the unreacted Ca metal is pushed out from the bottom layer to the top layer, forming a Ag-Ca solid solution with a high Ca content. The electrical conductivity of the top layer was decreased due to the incorporation of Ca, leading to less free-carrier scattering and higher optical transmittance.

An optimum Ag/Ca double layer with high transmittance and low electrical resistivity can be achieved if the surface coverage of the Ag layer is as low as possible while forming a continuous film. The Ag (7 nm)/Ca (20 nm) double layer shows transmittance of nearly 80% at a 500 nm wavelength and a sheet resistance of 13 $\Omega/\square$.

ACKNOWLEDGEMENT

REFERENCES

1. J. J. Lih, C. F. Sung, C. H. Li, T. H. Hsiao, and H. H. Lee, *J. Soc. Inform. Display* **12**, 367 (2004).
2. A. Nathan, S. Alexander, K. Sakariya, P. Servati, S. Tao, D. Striakhilev, A. Kumar, S. Sambandan, S. Jafarabadiashtiani, and Y. Vygranenko, *Proc. 4th IMID*, p. 343, Daegu (2004).
3. M. Kashiwabara, K. Hanawa, R. Asaki, I. Kobori, R. Matsuura, H. Yamada, T. Yamamoto, A. Ozama, Y. Sato, S. Terada, J. Yamada, T. Sasaoka, S. Tamura, and T. Urabe, *SID 04 Digest*, p. 1017, Seattle (2004).
4. S. T. Lee, B. D. Chin, M. H. Kim, T. M. Kang, M. W. Song, J. H. Lee, H. D. Kim, and H. K. Chung, *SID 04 Digest*, p. 1008, Seattle (2004).
5. L. S. Hung, C. W. Tang, M. G. Mason, P. Raychaudhuri, and J. Madathil, *Appl. Phys. Lett.* **78**, 544 (2001).
6. G. G. Andersson, M. P. de Jong, F. J. J. Janssen, J. M. Sturm, L. J. van IJzendoorn, A. W. Denier van der Gon, M. J. A. de Voigt, and H. H. Brongersma, *J. Appl. Phys.* **90**, 1376 (2001).
7. C. J. Lee, R. B. Pode, D. G. Moon, and J. I. Han, *Thin Solid Films* **467**, 201 (2004).
8. R. B. Pode, C. J. Lee, D. G. Moon, and J. I. Han, *Appl. Phys. Lett.* **84**, 4614 (2004).
9. D. G. Moon, R. B. Pode, C. J. Lee, and J. I. Han, *Materials Science and Engineering B* **121**, 232 (2005).
10. C. J. Lee, J. I. Han, and D. G. Moon, *Molecular Crystals and Liquid Crystals* **459**, 75 (2006).
11. D. G. Moon, R. B. Pode, C. J. Lee, and J. I. Han, *Synthetic Metals* **146**, 63 (2004).
12. C. J. Lee, R. B. Pode, J. I. Han, and D. G. Moon, *Appl. Phys. Lett.* **89**, 253508 (2006).
13. C. J. Lee, R. B. Pode, J. I. Han, and D. G. Moon, *Appl. Phys. Lett.* **89**, 123501 (2006).
14. S. J. Gregg and W. B. Jepson, *J. Chem. Soc.* 712 (1960).
15. R. H. Bube, *Electrons in Solids: an Introductory Survey*, 3rd ed., p. 154, Academic Press Inc. (1992).